Effect of αvβ3 Blockade Against Acute Lung Injury Induced by Influenza A Virus and Its Mechanism

Wendi Yu
Guangzhou University of Chinese Medicine
Maoseng Zeng
Guangzhou University of Chinese Medicine
Jinyuan Liu
Guangzhou University of Chinese Medicine
Huixian Wang
Guangzhou University of Chinese Medicine
peiping xu (xupeiping@gzucm.edu.cn)
Guangzhou University of Chinese Medicine https://orcid.org/0000-0002-6720-7327

Research Article

Keywords: Cyclo(RGDyK), Acute lung injury, Influenza A virus, Viral pneumonia, αvβ3/TGF-β1/HIF-1α signaling pathway

Posted Date: May 27th, 2021

DOI: https://doi.org/10.21203/rs.3.rs-545939/v1

Abstract

Integrin αvβ3 is a heterodimer formed by αv and β3 subunits that is expressed in pulmonary endothelial cells, alveolar epithelial cells, interstitial cells and macrophages. Integrin αvβ3 not only has a common role of integrin family molecules in inflammation and tissue fibrosis, but also mediates the adsorption and penetration of various viruses into susceptible cells. Nevertheless, there are few studies on the effect of αvβ3 on acute lung injury (ALI) induced by influenza virus and its mechanism. Here, the effects of αvβ3 blockade [Cyclo(RGDyK)] against ALI induced by influenza A virus (IAV) *in vitro* and *in vivo* and its possible mechanism were studied. A549 cells and mice were infected with influenza virus A/FM/1/47 to induce ALI *in vitro* and *in vivo*. The results showed that Cyclo(RGDyK) reduced the ALI induced by IAV, alleviated pulmonary edema, improved lung histopathological changes and alleviated the accumulation of inflammatory cells in the lung. Cyclo(RGDyK) had inhibitory effect on cells and mice infected by IAV. Cyclo(RGDyK) (150 μg/kg) showed effective antiviral activity *in vivo*. Cyclo(RGDyK) had 70% protective effect against IAV and effectively reduced virus titer and inflammation in lung tissue. Cyclo(RGDyK) exhibited significantly anti-inflammatory and anti-fibrotic effect on improving the pneumonia and degree of pulmonary fibrosis and reducing the levels of pulmonary fibrotic markers (LN, HA, PCIII, IV-C, TGF-β1, and α-SMA). Additionally, Cyclo(RGDyK) inhibited expression of αvβ3,TGF-β1, HIF-1α, NF-κB, and p38 MAPK in the cells and mice lung tissues. The results showed that Cyclo(RGDyK) had a protective effect on ALI in mice infected with IAV and inhibited the progress of lung inflammation and fibrosis, which may be concern with its regulation of αvβ3/TGF-β1/HIF-1α signaling pathway.

1. Introduction

Influenza is an infectious disease caused by influenza virus that threatens global public health and sometimes leads to pandemics[1]. Influenza virus often causes acute lung injury (ALI) and promote pulmonary fibrosis, which can lead to acute respiratory distress syndrome (ARDS)[2, 3]. At present, there is still a shortage of effective drugs to curb viral ALI/ARDS. Antiviral drugs may have an effect in the early stage of viral infection, but the effect on severe pneumonia lung injury in the late stage of viral infection is limited, and resistance to antiviral therapy is increasing[4].

Extracellular matrix (ECM) proteins, such as fibronectin, collagen, and laminin, interact with integrins, transduce signals to regulate cell growth, differentiation, migration, and other cellular activities[5]. Integrins are cell surface glycoproteins involved in cell-cell and cell-matrix interactions. They are composed of an α and a β subunit [6]. They serve as an entry receptor for various viruses, such as herpesviruses and Epstein-Barr virus[7, 8]. Diffuse alveolar injury caused by inflammation is central to the pathophysiology of ALI[9]. Integrins on leukocytes are upregulated in response to various cytokines and chemokines, and affect the progression and prognosis of many inflammatory processes[10]. It is worth noting that integrin αv plays a key role in the formation of inflammatory microenvironment by regulating expression of cytokines and matrix components[11, 12].

The activation of transforming growth factor (TGF)-β in epithelial cells is a central pathway in the pathogenesis of pulmonary fibrosis [13].Influenza A virus (IAV) neuraminidase (NA) can activate TGF-β activation by removing sialic acid motifs from latent TGF-β[14, 15]. The latent TGF-β complex contains an arginine-glycine-aspartic acid (RGD) sequence motif, which directly binds to and activates the following integrins: αvβ3, αvβ5, αvβ6 and αvβ8[16], and leads to the release of TGF-β from the ECM, and biological activation[17]. Integrin and TGF-β play a key role in the process of inflammation by inducing the release of inflammatory mediators[18]. Therefore, intervening in the intergin and TGF-β signaling pathway can reduce inflammation, which is a potential therapeutic strategy for ALI[19].

The integrin family are cell surface receptor glycoproteins that are widely expressed in most cells. Integrin is a heterodimer composed of nine β subunits and 18 α subunits, which constitute ≥ 20 integrins according to different combinations[20]. Studies have shown that integrins can regulate the release of inflammatory cytokines and alveolar capillary permeability, which is a new target for anti-inflammatory therapy[21]. Integrins are also involved in the formation of collagen fibers[3, 22]. Integrin αvβ3 is a receptor for vitronectin. It is expressed on the lumen and vesicle surface of cultured endothelial cells and in resting rat pulmonary microvessels [23]. Integrin αvβ3 is also found in large blood vessels, human lung airway epithelium, neutrophils and monocytes[24]. Integrin αvβ3 promotes monocyte migration and participates in neutrophil migration on the ECM[25] .

Given the higher expression of integrin αvβ3 in acute lung inflammation [26], we hypothesize that αvβ3 upregulation during influenza infection is important for pathogenesis of viral ALI. Application of anti-αvβ3 blocking antibodies may play a major role in ALI. The aim of this study was to evaluate the antiviral activity of αvβ3 blockade [Cyclo(RGDyK)] against ALI induced by IAV and its mechanism.

2. Materials And Methods

2.1. Reagents, antibodies and animal

Cyclo(RGDyK) was purchased from Selleckchem (Houston, TX,USA), purity ≥ 99%. Oseltamivir carboxylate was purchased from Beyotime (Shanghai, China). These compounds prepared as dimethyl sulfoxide stock solution were diluted in the culture medium before being added to the cells and added at the required concentration during the culture. Anti-HIF-1αprimary antibodies were purchased from Cohesion Biosciences Limited (Suzhou, China).Anti-αvβ3 primary antibodies and anti-TGF-β1 primary antibodie were obtained from Beyotime (Shanghai, China). The neuraminidase Assay Kit was purchased from Beyotime (Shanghai, China). Specific pathogen free BALB/c mice, weighing 13-15g, were obtained from Guangdong Medical Experimental Center (Guangdong, China). Studies conform to the ethical standards of animal experiments approved by the animal protection and Welfare Committee of Guangzhou University of Chinese Medicine (Guangzhou, China). Study complies with regulations for the administration of affairs concerning experimental animals of Guangdong Province (2010, No. 41).

2.2. Cell Culture and Treatment

Human lung adenocarcinoma epithelial cells (A549) were purchased from the American Type Culture Collection (ATCC, Manassas, VA, USA). Cells were maintained in Dulbecco modified eagle's medium (DMEM), supplemented with 10% fetal bovine serum and 1% antibiotic (100 U/ml penicillin, 0.1 mg/ml streptomycin) with L-glutamine, and cultured in a humidified atmosphere with 5% CO_2 at 37 ℃. IAV strain A/FM/1/47 (H1N1) was acquired from ATCC. Influenza virus (1MOI) was inoculated on a 6-well plastic plate at 37 ℃ for 2 h, and then washed three times with PBS. After that, a series of concentrations of Cyclo(RGDyK) were carefully added to the cells and cultured at 37 ℃ for 48 hours. DMSO vehicle control was included in these experiments. Then, the supernatants were collected at 72 hpi, and the CPE of virus-infected cells were observed by microscope. Cells viability was assayed by 3-[4,5-dimethyl-thiazol-yl]-2,5-diphenyltetrazolium bromide(MTT). Aabsorbance was measured by microplate reader (Bio-Tek ELx800, Winooski, Vermont, USA) at 490 nm.

2.3. Reverse transcription and real-time quantitative PCR

Total RNA was reverse transcribed into cDNA using PrimeScript™ 1st Strand cDNA Synthesis Kit (Takara, Japan) according to the Manufacturer's protocol. M gene of A/FM/1/47 H1N1 was carried out as mentioned before[27]. IFV quantity of PCR products were analyzed in the light of the mode for normalized expression ($2^{-\triangle\triangle ct}$)[28]. Relative quantities (RQ) of influenza viral load in lung levels were normalized to the results of negative control group as 1.

2.4. Analysis of neuraminidase activity

NA enzymatic activity assay was performed as previously described [29] and samples were analyzed according to the neuraminidase assay kit manufacturer's instructions(Beyotime Institute of Biotechnology, Haimen, Jiangsu, China). Briefly, Cells were infected with virus (FM1/H1N1, 1MOI), and Cyclo(RGDyK) for 72 h. Cells were resuspended in 10 mL assay buffer and were mixed with 70 mL detection buffer, 10 mL NA fluorogenic substrate and 10 mL water. Cleavage of the fluorogenic substrate from NA produces fluorescence was measured using a Synergy™ HT Multi-detection microplate reader (BioTek Instruments, Inc, Winooski,Vermont, USA) at an emission wavelength of 450 nm and an excitation wavelength of 322 nm. The fluorescence intensity represents the activity of NA, which is quantified as the fluorescence above the background values (negative control).

2.5. Western blot

Cells were infected with IAV (1 MOI) and αvβ3, TGF-β1, HIF-1α, NF-κB p65, p38MAPK was detected at 72h pi. Western blot analysis was performed with a SDS-PAGE electrophoresis system as mentioned before[30]. The membrane was then incubated overnight at 4 ℃ with the following primary antibodies, HIF-1α (1:1000), TGF-β1 (1:500), NF-κB p65 (1:500), αvβ3 (1:500), p38MAPK (1:500), and GADPH (1:5,000). Protein levels were normalized to GADPH as an untreated control. Western blots were quantified using standard densitometry analysis (ImageJ software).

2.6. ELISA

Concentrations of MCP-1, TGF-β1, HIF-1α, IL-6, IL-1β, IFN-γ and TNF-α in the supernatant were measured according to the instructions of ELISA kit manufacturer (Shanghai Enzyme-linked Biotechnology Co., Ltd, Shanghai,China). Optical density(OD_{450nm}) was read by an ELISA plate reader (Bio-Tek ELx800, Winooski, Vermont, USA).

2.7. Therapeutic efficacy in mice

Mice were anesthetized and intranasal challenged with 5×LD_{50} doses of FM1/ H1N1 in sterile phosphate-buffered saline (PBS pre-cooled). On the basis of previous studies, the dosage of Cyclo(RGDyK) in mice as determined according to previous studies[31].After infection, mice were given Cyclo(RGDyK) (150μg/kg, intraperitoneal injection) and monitored for 15 days after infection to observe signs of toxicity and death and to assess survival rate and time. On day 6 post-infection, the mice were killed and lung samples were collected for the detection of relevant indicators. Body weight and wet weight of the lungs were measured. Lung index was calculated as previously described[32].

2.8. Hematoxylin and eosin (HE) and Masson Trichrome Staining

Lung specimens were fixed in 10% formalin, embedded in paraffin, cut into 5 μm sections and stained with hematoxylin and eosin (HE) or Masson's trichrome using routine histopathological methods as described previously[33]. 5 μm sections were stained with HE or Masson's trichrome staining and observed under light microscope. Histopathological score was between 0 (normal) and 5 (severe) based on the following pathological conditions: congestion,edema, polymorphonuclear leukocyte and monocyte infiltration, necrosis and hemorrhage as previously described[34]. Randomly selected areas of lung sections were examined by light microscopy at magnifications of ×100, ×200 and ×400 (Chongqing Optech Instruments Co., Chongqing, China). All histological analyses were performed by experienced pathologists who were blinded to the respective treatments. Collagen deposition was also assessed by Masson's trichrome staining. Ten randomly selected images focused on the central vein were analyzed for the extent of fibrosis using an image analysis system (Image Pro Plus version 6.0, Media Cybernetics, MD, USA). The results were expressed as integral optical density values (IOD).

2.9. Electron microscopy examination of lung tissue

Lung was fixed in 2.5% glutaraldehyde and 1% osmic acid, dehydrated and dried, and observed by scanning electron microscopy (SEM 1430 VP; LEO Electron Microscopy Ltd., Oberkochen, Germany).

2.10. Immunohistochemical analysis

Twelve hours after the last administration at day 5, mice were sacrificed to collect the lungs. Mouse lungs were excised, fixed in 10% formaldehyde for at least 24 hours, dehydrated in graded ethanol, and embedded in paraffin. Five-micrometer sections were stained with hematoxylin–eosin. Expression of αvβ3, HIF-1α and TGF-β1 in tracheal mucosa was determined by immunohistochemistry (IHC). Immunohistochemical staining was performed for αvβ3, HIF-1α and TGF-β1 antibody (Beyotime,Shanghai, China) was performed manually using goat anti-rabbit IgG Antibody Kit (Boster).

Images were captured using the same magnification (40×/0.75) with an Olympus (HB-2) camera (Olympus Corporation, Tokyo, Japan). Protein labeling intensity measurements were expressed as integrated optical density (IOD) and were performed on six randomly selected sections using the Image-Pro Plus 6.0 image analysis system (Media Cybernetics Inc., Rockville, MD, USA).

2.11. ELISA assay for lung fibrotic markers

Serum levels of alpha-smooth muscle actin (α-SMA), laminin (LN), hyaluronic acid (HA), procollagen type III (PCIII), collagen type IV (IV-C) and TGF-β1 were measured by ELISA kit (Shanghai Enzyme-linked Biotechnology Co., Ltd. ,Shanghai, China). The test was carried out according to the manufacturer's instructions.

2.12. Measurement of inflammatory parameters in lung of IAV-infected mice

Levels of MCP-1,TNF-α, IL-6, IL-1β and IFN-γ in lung tissue were detected by ELISA method in the light of the manufacturer's instructions (Shanghai Enzyme-linked Biotechnology Co., Ltd. ,Shanghai, China) by ELISA plate reader (Bio-Tek ELx800, Winooski, Vermont, USA).

2.13. Statistical analysis

Data are expressed as the mean ± S.D. and statistically significant difference was analyzed by SPSS18.0 software (SPSS Inc., Chicago, IL, USA). The comparison between the two groups was conducted by Student’s t-test. Differences were considered statistically significant at $p < 0.05$.

3. Results

3.1. Anti-influenza abilities of Cyclo (RGDyK) in vitro

MTT assay showed that Cyclo(RGDyK) (0.125-2M) increased cell survival in a dose-dependent manner (Fig. 1A). In addition, Cyclo(RGDyK) at concentrations of 10–40 nM significantly inhibited the expression of the M gene (Fig. 1B). In addition, Cyclo(RGDyK) at 10–40 nM almost completely inhibited neuraminidase activity compared to oseltamivir (Fig. 1C). The results suggest that Cyclo(RGDyK) can inhibit neuraminidase activity and viral load and protect cells from viral infection.

3.2. Effects of Cyclo(RGDyK) on cytokines production in cells infected by IAV

As shown in Figs. 2 and 3, influenza virus infection increases the levels of HIF-1α,TGF-β1,IL-1β,MCP-1, IFN-γ and TNF-α in the cells. Cyclo(RGDyK) (10-40nM) inhibited the over secretion of cytokines in a dose-dependent manner.

3.3. Effects of Cyclo(RGDyK) on the expression of p38MAPK,NF-κB,αvβ3, TGF-β1 and HIF-1α in cells induced by IAV

As shown in Fig. 9, the expression levels of p38MAPK and NF-κB in IAV-C group were significantly higher than those in the NC group ($p < 0.001$) (Fig. 4A-B,D). Compared with IAV-C group, the expression of p38MAPK and NF-κB in cells treated with 10-40nM Cyclo(RGDyK) were decreased ($p < 0.01$) (Fig. 4A,C-D). These results indicate that Cyclo(RGDyK) can inhibit the expression of p38MAPK and NF-κB in cells induced by influenza virus.

Compared with NC group, the expression levels of αVβ3, HIF-1α and TGF-β1 in the cells of IAV-C group were significantly increased. After administration of Cyclo (RGDyK), the expression of αVβ3, HIF-1α and TGF-β1 was significantly reversed in cells ($p < 0.01$) (Fig. 4A-B,E-F).

3.4. Anti-influenza activity of Cyclo(RGDyK) in IAV-infected mice.

Evaluation of the protective effect of Cyclo(RGDyK) on influenza A (H1N1) mice by survival rate and lung index. In this study, Cyclo(RGDyK) (150μg/kg) can reduce the inflammatory response of lung tissue in mice. The lung index of IAV-C group was 1.58 ± 0.18, while that of Cyclo(RGDyK) groups were 1.11 ± 0.15 (Fig. 5A), which suggested that Cyclo(RGDyK) can effectively reduce the lung index ($p < 0.05$). Cyclo(RGDyK) can effectively prolong the survival time of infected mice (Fig. 5B) and decline viral load in lung(Fig. 5C).Cyclo(RGDyK) at doses of 150 μg/kg protected 70% of mice from lethal infection, respectively (Fig. 5D). These results demonstrate that Cyclo(RGDyK) exhibited a protective effect on influenza-infected mice.

3.5. Effect of Cyclo(RGDyK) on pathological changes of lung tissue in ALI mice induced by IAV

In the NC group, no evident histological alteration was observed in lung specimens, intact alveoli and lung bronchus structure, no exudates in the bronchial and bronchiolar lumina (Fig. 6A). In IAV-C group, there were obvious ALI, such as a large number of neutrophils infiltration around the lung interstitium, a large amount of exudation in the bronchioles, marked infiltration of neutrophils in the bronchioles, and obvious swelling of the alveolar wall (Fig. 6B). In mice treated with Cyclo(RGDyK) (150μg/kg), these lesions were

improved to varying degrees (Fig. 6C-D), suggesting that Cyclo(RGDyK) can protect against ALI induced by IAV.

3.6. Ultrastructural changes of lung tissue by electron microscope

Electron microscopic observation showed that the alveolar structure in NC group was normal, no abnormal exudate in the alveolar cavity,and the morphology of type II alveolar epithelial cells was normal (Fig. 7A). In IAV-C group, the lung tissue had different degrees of pathological changes, such as the proliferation and swelling of alveolar epithelial type II cells, a large amount of exudate in the alveolar cavity, including a large number of inflammatory cells,such as monocytes, lymphocytes, etc. A large number of collagen forming cells (such as fibroblasts, smooth muscle cells, etc.) could be seen in the alveolar septum and a large number of collagen fibers and elastic fibers proliferated, forming obvious cord like fibers crisscross(Fig. 7B). In mice treated with Cyclo(RGDyK) (150μg/kg), these lesions,such as the number and volume of alveolar epithelial cells, exudates and mononuclear phagocytes in alveoli, collagen fibers in the alveolar septum, and honeycomb structure of lung were improved to varying degrees (Fig. 7C), indicating that Cyclo(RGDyK) protects against ALI induced by IAV.

(A) Ultrastructural changes of lung tissues in NC group; (B) Ultrastructural changes of lung tissues in IAV-C group; (C) Ultrastructural changes of lung tissues in Cyclo (RGDyK) group. n = 5 mice per group.

3.7. Effect of Cyclo(RGDyK) on collagen changes in lung tissue of ALI mice induced by IAV

The histopathological abnormalities of the lung were studied by Masson's trichrome staining. Masson staining showed no collagen deposition, necrosis, inflammation and fibrosis in the lung tissue of NC group (Fig. 8A). In IAV-C group, inflammatory cell infiltration and collagen deposition were obvious(Fig. 8B). However, 150 μg/kg Cyclo(RGDyK) can significantly improve the structure and degree of pulmonary fibrosis, and significantly reduce the area density percentage of collagen deposition ($p < 0.05$) (Figure.8C-D).

3.8. Effects of Cyclo(RGDyK) on levels of lung fibrotic markers in ALI mice induced by IAV

The levels of TGF-β1 in serum and α-SMA in lung tissue of IAV-C group were significantly higher than those of NC group ($p < 0.05 – 0.001$, Fig. 9A-B), but Cyclo (RGDyK) treatment (150 μg/kg) significantly decreased the levels of these markers ($p < 0.05$ or 0.01, Fig. 9A-B).

There were significant differences in serum LN, HA, PCIII and IV-C between IAV-C group and NC group ($p < 0.01$). Cyclo(RGDyK) (150 μmg/kg) significantly inhibited the increase of these markers induced by IAV (Fig. 9C-E).

3.9. Effects of Cyclo(RGDyK) on cytokines production in lung tissue of ALI mice induced by IAV

Influenza virus induced lung inflammation and subsequent ALI are closely related to the over secretion of a variety of proinflammatory cytokines. IL-1β, MCP-1, IFN-γ, IL-6 and TNF-α are key pro-inflammatory cytokines in the process of inflammation. Therefore, we studied the expression of these pro-inflammatory cytokines in lung tissue. As shown in Fig. 10, influenza virus infection increases the levels of IL-1β, MCP-1, IFN-γ, and TNF-α in the lungs of mice. Cyclo(RGDyK) (150 μg/kg) inhibited the over secretion of pro-inflammatory cytokines in a dose-dependent manner.

3.10. Effects of Cyclo(RGDyK) on the expression of αvβ3, TGF-β1 and HIF-1α lung tissue of ALI mice induced by IAV

As shown in Fig. 10–12, the expression levels of αvβ3, TGF-β1 and HIF-1α in IAV-C group were significantly higher than those in NC group ($p < 0.001$) (Fig. 11–13). Compared with IAV-C group, the expression of αvβ3, TGF-β1 and HIF-1α in the lung of mice treated with 150 μg/kg Cyclo(RGDyK) were decreased ($p < 0.01$) (Fig. 11-13D). These results indicate that Cyclo(RGDyK) can inhibit the expression of αvβ3, TGF-β1 and HIF-1α induced by influenza virus.

4. Discussion

Viral lung injury is a kind of pathological lung injury caused by virus infection. Novel coronaviruses, IAV H1N1, severe acute respiratory syndrome coronavirus, IAV H5N1, IAV H7N9 and other viruses can ALI and ARDS [35, 36]. Influenza virus is a single-stranded RNA virus that causes acute respiratory infecctions. IAV infection often leads to ALI and pulmonary fibrosis and ARDS[37, 38]. At present, there is still a shortage of effective drugs to control viral ALI/ARDS[4]. Therefore, it is important to develop new targeted drugs for the treatment of these diseases.

Integrin αvβ3 plays a critical role in fibrosis and inflammation. However, the effect of αvβ3 on ALI induced by IAV is still unclear. This study evaluated the anti-viral activity of αvβ3 blockade against ALI induced by

IAV, and its mechanism of action. The results showed that influenza virus infection led to inflammation and increased levels of fibrosis and collagen in mice. The αvβ3 blockade with Cyclo(RGDyK) significantly inhibited all these inflammatory and fibrotic changes, suggesting that Cyclo(RGDyK) can reduce lung inflammation and fibrosis induced by IAV. Cyclo(RGDyK) also significantly improved lung tissue morphology, reduced pulmonary fibrosis score, and inhibited expression of αvβ3, TGF-β1, NF-κB p65, p38MAPK and HIF-1α. These results confirmed the beneficial effect of Cyclo(RGDyK) on ALI and pulmonary fibrosis induced by influenza virus.

The exact pathogenesis of ALI induced by IAV has not been fully elucidated[39][39][39].Cytokine storm is an important cause of uncontrollable inflammation caused by virus infection[40]. Severe types of pneumonia lead to lung ischemia and hypoxia, and eventually to irreversible ARDS[41]. Therefore, viral lung injury (ALI/ARDS) is almost always associated with lung inflammation and fibrosis[42].Our study showed that the main symptoms of ALI and ARDS in mice infected with IAV were inflammation and collagen deposition. The surviving infected mice developed severe fibrosis, including typical interstitial and alveolar fibrosis, alveolar wall thickening, tissue expansion, bronchiolar wall thickening, and fibroblast proliferation.

The p38MAPK and NF-κB are the key signaling pathways for the expression of inflammatory cytokines and play a key role in the development of ALI[43]. NF-κB is closely related to inflammation and tissue fibrosis. NF-κB activation can induce the production of inflammatory factors, such as IL-1β, IL-6, TNF-α and TGF-β1, and then lead to lung inflammation and fibrosis. In this study,we found that influenza virus infection increased the production of proinflammatory cytokines in lung, including IL-1β, IL-6, IFN-γ, MCP-1 and TNF-α, and up-regulated expression of NF-κB and p38 MAPK, which was reversed by Cyclo(RGDyK) treatment. These results suggested that Cyclo(RGDyK) alleviated influenza-virus-induced pneumonia and fibrosis in mice by inhibiting NF-κB and p38 MAPK-mediated pro-inflammatory signaling cascade.

Lung inflammation and fibrosis were measured in experimental and clinical studies using four indicators: HA, LN, IV-C and PCIII[44]. In this study, the serum levels of all four markers were significantly reduced by Cyclo(RGDyK) treatment compared with the IAV-C group, indicating that Cyclo(RGDyK) reduced the serum levels of LN, HA, IV-C and PCIII in mice with pulmonary fibrosis.

TGF-β is a regulatory factor by controlling the occurrence and regression of inflammatory response and the occurrence and maintenance of fibrosis[45]. Intervention in TGF-β signaling pathway can reduce inflammation, which is considered as a potential target for the treatment of ALI/ARDS[45]. Influenza virus NA can directly activate latent TGF-β[43]. When mice were infected with influenza virus, the activity of TGF-β increased. TGF-β1 accelerates the process of inflammation by inducing the release of inflammatory mediators, including IL-6 and IL-17[46]. Our study also showed that the levels of TGF-β1, TNF-α, IL-6, IL-1 β and TGF-β1 were increased in cells and mice infected with influenza virus. The Cyclo(RGDyK) could inhibit the levels of inflammatory cytokines induced by influenza virus.

Hypoxia inducible factor (HIF) is a heterodimer transcription factor, which is composed of HIF-1α (or its analogs, HIF-2α and hif-3α) and HIF-1β subunit, and is the target gene for hypoxia adaptation and

inflammation development. The control element of HIF is mainly HIF-1[47]. HIF-1α is an important therapeutic target to control inflammation and fibrosis, and plays an important role in ALI[48]. Hypoxia induced HIF-1α gene expression and enhanced expression of α-SMA, TGF-β1 and Smad2[49]. HIF-1α is involved in the regulation of inflammatory factors such as TNF-α, IL-6 and IL-10[50], and IL-6 and TNF-α play an important role in the production and development of cytokine storm[51]. The expression of HIF-1α in lung tissue was up-regulated by local hypoxia induced by influenza virus pneumonia [52]. Our study also showed that the level of HIF-1α in cells and mice infected with influenza virus increased, while αvβ3 inhibitor Cyclo(RGDyK) effectively reduced expression of HIF-1α in cells and mice.

Integrin αvβ3 is a heterodimer formed by αv and β3 subunits that is expressed in pulmonary endothelial cells, alveolar epithelial cells, interstitial cells and macrophages[21]. Integrin αvβ3 not only has the common role of integrin family molecules in inflammation and tissue fibrosis, but also can mediate the adsorption and penetration of a variety of viruses into susceptible cells[23, 53].

In particular, hypoxia is an important factor to increase the expression of αvβ3. Hypoxia can increase the mRNA production of αvβ3 in endothelial cells, but has no effect on αvβ5[54].After IAV infection, mice had acute lung inflammation, fibrosis and other lung injury lesions. Severe pneumonia and other diseases produced local hypoxia in lung tissue. In our previous work, we studied the expression of αvβ3 in mice with influenza-virus-induced lung injury. We found that influenza virus induced expression of αvβ3 in cells and mice. Moreover, severe pneumonia caused by influenza virus infection produced local hypoxic lung environment. Hypoxia increased expression of αvβ3 mRNA in endothelial cells[54].Our work showed that the expression levels of αvβ3, HIF-1α and TGF-β1 protein in lung tissue increased after IAV infection. Cyclo(RGDyK) inhibited viral pneumonia and reduce inflammatory factors and fibrocytokines in blood and lung tissue. These results indicated that αvβ3, TGF-β1 and HIF-1α and their signaling pathways were involved in the pathochemical process of virus infection, inflammation and tissue fibrosis. These abnormal functions and pathological changes were reduced by inhibiting αvβ3 signal, suggesting that Cyclo(RGDyK) improved lung inflammation and collagen deposition by inhibiting the expression levels of αvβ3, HIF-1α and TGF-β1.

5. Conclusions

In conclusion, Cyclo(RGDyK) had a protective effect on ALI in mice infected with influenza virus, and inhibited the progress of lung inflammation and fibrosis, which may be related to its regulation of the αvβ3/TGF-β1/HIF-1α signaling pathway. This finding provided a new perspective for understanding the effect of αvβ3 on ALI induced by IAV. More studies are needed to study the pathogenesis of viral ALI and the mechanism of αvβ3 on viral ALI, which may provide evidence for the treatment of viral diseases.

Declarations

Declaration of Competing Interest

The authors declare that they have no known competing financial interests or personal relationships that could have appeared to influence the work reported in this paper.

Ethical approval All the studies conform to the ethical standards of animal experiments approved by the animal protection and Welfare Committee of Guangzhou University of Chinese Medicine (Guangzhou, China). Humane endpoints are chosen in the experimental animals (e.g. *in vivo* study) via euthanasia and use of anesthesia (Euthanasia of mice under anesthesia with 3% pentobarbital and virus inoculation under anesthesia with ether inhalation). This study complies with regulations for the administration of affairs concerning experimental animals of Guangdong Province (2010, No. 41)

Author's contribution

All authors have contributed substantially to the design and execution of this study and approve the final version of this manuscript. Miss Wendi Yu performed the presented experiments and wrote the manuscript. Dr. Jinyuan Liu conducted histopathological study and image analysis. Miss Maosen Zeng and Huixian Wang conducted experiments and analyzed data. Prof. Peiping Xu designed the presented experiments and revised the manuscript. All authors read and approved the manuscript.

Data availability

The datasets generated during and/or analysed during the current study are available from the corresponding author on reasonable request.

Acknowledgments

We thank International Science Editing (Co. Clare, Ireland) for the language editorial assistance in the preparation of the manuscript.

References

1. Eccles, R. 2005. Understanding the symptoms of the common cold and influenza. *Lancet Infect Dis* 5: 718–725.
2. Qiao, J., M. J. Zhang, J. M. Bi, X. Wang, G. C. Deng, G. M. He, Z. H. Luan, N. N. Lv, T. Xu, and L. H. Zhao. 2009. Pulmonary fibrosis induced by H5N1 viral infection in mice. Resp Res *10*.
3. Jolly, L., A. Stavrou, G. Vanderstoken, V. A. Meliopoulos, A. Habgood, A. L. Tatler, J. Porte, A. Knox, P. Weinreb, and S. Violette, et al. 2014. Influenza Promotes Collagen Deposition via alpha v beta 6 Integrin-mediated Transforming Growth Factor beta Activation. *J Biol Chem* 289: 35246–35263.
4. Zhang, Q., T. Z. Liang, K. S. Nandakumar, and S. W. Liu. 2020. *Emerging and state of the art hemagglutinin-targeted influenza virus inhibitors*. Expert Opin Pharmaco.

5. McCullers, J. A. 2014. The co-pathogenesis of influenza viruses with bacteria in the lung. *Nat Rev Microbiol* 12: 252–262.
6. ffrench-Constant, C., and H. Colognato. 2004. Integrins: versatile integrators of extracellular signals. *Trends Cell Biol* 14: 678–686.
7. Stewart, P. L., and G. R. Nemerow. 2007. Cell integrins: commonly used receptors for diverse viral pathogens. *Trends Microbiol* 15: 500–507.
8. Chesnokova, L. S., S. L. Nishimura, and L. M. Hutt-Fletcher. 2010. Fusion of epithelial cells by Epstein-Barr virus proteins is triggered by binding of viral glycoproteins gHgL to integrins alpha v beta 6 or alpha v beta 8 (vol 106, pg 20464, 2009). P Natl Acad Sci USA *107*, 3275–3275.
9. Weinacker, A. B., and L. T. Vaszar. 2001. Acute respiratory distress syndrome: Physiology and new management strategies. *Annu Rev Med* 52: 221–237.
10. Lundberg, S., J. Lindholm, L. Lindbom, P. M. Hellstrom, and J. Werr. 2006. Integrin alpha 2 beta 1 regulates neutrophil recruitment and inflammatory activity in experimental colitis in mice. Gastroenterology *130*, A347-A347.
11. Luzina, I. G., N. W. Todd, N. Nacu, V. Lockatell, J. Choi, L. K. Hummers, and S. P. Atamas. 2009. Regulation of Pulmonary Inflammation and Fibrosis Through Expression of Integrins alpha V beta 3 and alpha V beta 5 on Pulmonary T Lymphocytes. *Arthritis Rheum-Us* 60: 1530–1539.
12. Acharya, M., S. Mukhopadhyay, H. Paidassi, T. Jamil, C. Chow, S. Kissler, L. M. Stuart, R. O. Hynes, and A. Lacy-Hulbert. 2010. alpha v Integrin expression by DCs is required for Th17 cell differentiation and development of experimental autoimmune encephalomyelitis in mice. *J Clin Invest* 120: 4445–4452.
13. Fernandez, I. E., and O. Eickelberg. 2012. New cellular and molecular mechanisms of lung injury and fibrosis in idiopathic pulmonary fibrosis. *Lancet* 380: 680–688.
14. Carlson, C. M., E. A. Turpin, L. A. Moser, K. B. O'Brien, T. D. Cline, J. C. Jones, T. M. Tumpey, J. M. Katz, L. A. Kelley, and J. Gauldie, et al. 2010. Transforming Growth Factor-beta: Activation by Neuraminidase and Role in Highly Pathogenic H5N1 Influenza Pathogenesis. Plos Pathog *6*.
15. Li, N., A. H. Ren, X. S. Wang, X. Fan, Y. Zhao, G. F. Gao, P. Cleary, and B. N. Wang. 2015. Influenza viral neuraminidase primes bacterial coinfection through TGF-beta-mediated expression of host cell receptors. *P Natl Acad Sci USA* 112: 238–243.
16. Goodwin, A., and G. Jenkins. 2009. Role of integrin-mediated TGF beta activation in the pathogenesis of pulmonary fibrosis. *Biochem Soc T* 37: 849–854.
17. Yang, Z. W., Z. Y. Mu, B. Dabovic, V. Jurukovski, D. W. Yu, J. Sung, X. Z. Xiong, and J. S. Munger. 2007. Absence of integrin-mediated TGF beta 1 activation in vivo recapitulates the phenotype of TGF beta 1-null mice. *J Cell Biol* 176: 787–793.
18. Ichimaru, Y., D. I. Krimmer, J. K. Burgess, J. L. Black, and B. G. G. Oliver. 2012. TGF-beta enhances deposition of perlecan from COPD airway smooth muscle. *Am J Physiol-Lung C* 302: L325–L333.
19. Yang, Z. S., J. Y. Yan, N. P. Han, W. Zhou, Y. Cheng, X. M. Zhang, N. Li, and J. L. Yuan. 2016. Anti-inflammatory effect of Yu-Ping-Feng-San via TGF-beta 1 signaling suppression in rat model of

COPD. *Iran J Basic Med Sci* 19: 993–1002.

20. Baldwin, H. S., and C. A. Buck. 1994. Integrins and Other Cell-Adhesion Molecules in Cardiac Development. *Trends Cardiovas Med* 4: 178–187.
21. Ding, X. B., X. Wang, X. Zhao, S. Q. Jin, Y. Tong, H. Ren, Z. X. Chen, and Q. Li. 2015. Rgd Peptides Protects against Acute Lung Injury in Septic Mice through Wisp1-Integrin Beta 6 Pathway Inhibition. Shock *43*, 352–360.
22. Hogmalm, A., D. Sheppard, U. Lappalainen, and K. Bry. 2010. beta 6 Integrin Subunit Deficiency Alleviates Lung Injury in a Mouse Model of Bronchopulmonary Dysplasia. *Am J Resp Cell Mol* 43: 88–98.
23. Singh, B., C. Z. Fu, and J. Bhattacharya. 2000. Vascular expression of the alpha(v)beta(3)-integrin in lung and other organs. *Am J Physiol-Lung C* 278: L217–L226.
24. Chung, T. W., M. J. Park, H. S. Kim, H. J. Choi, and K. T. Ha. 2016. Integrin alpha V beta 3 and alpha V beta 5 are required for leukemia inhibitory factor-mediated the adhesion of trophoblast cells to the endometrial cells. *Biochem Bioph Res Co* 469: 936–940.
25. Weerasinghe, D., K. P. McHugh, F. P. Ross, E. J. Brown, R. H. Gisler, and B. A. Imhof. 1998. A role for the alpha v beta 3 integrin in the transmigration of monocytes. *J Cell Biol* 142: 595–607.
26. Janardhan, K. S., G. D. Appleyard, and B. Singh. 2004. Expression of integrin subunits alpha v and beta 3 in acute lung inflammation. *Histochem Cell Biol* 121: 383–390.
27. Liao, S. H., Y. Li, Y. N. Lai, N. Liu, F. X. Zhang, and P. P. Xu. 2017. Ribavirin attenuates the respiratory immune responses to influenza viral infection in mice. *Arch Virol* 162: 1661–1669.
28. Livak, K. J., and T. D. Schmittgen. 2001. Analysis of relative gene expression data using real-time quantitative PCR and the 2(T)(-Delta Delta C) method. *Methods* 25: 402–408.
29. Wang, S., H. Li, Y. H. Chen, H. T. Wei, G. F. Gao, H. Q. Liu, S. L. Huang, and J. L. Chen. 2012. Transport of Influenza Virus Neuraminidase (NA) to Host Cell Surface Is Regulated by ARHGAP21 and Cdc42 Proteins. *J Biol Chem* 287: 9804–9816.
30. Ye, Y., H. X. Wang, J. Y. Liu, F. Zhao, and P. P. Xu. 2020. Polygalasaponin F treats mice with pneumonia induced by influenza virus. *Inflammopharmacology* 28: 299–310.
31. Tannous, B., T. Tian, and P. Obeid. 2018. Efficient Delivery of Sirnas to Glioma Via Functionalized Extracellular Vesicles Primed by Radiation. *Neuro-Oncology* 20: 100–100.
32. Li, Y., Y. N. Lai, Y. Wang, N. Liu, F. X. Zhang, and P. P. Xu. 2016. 1, 8-Cineol Protect Against Influenza-Virus-Induced Pneumonia in Mice. Inflammation *39*, 1582–1593.
33. Ho, L. T. Y., N. Skiba, C. Ullmer, and P. V. Rao. 2018. Lysophosphatidic Acid Induces ECM Production via Activation of the Mechanosensitive YAP/TAZ Transcriptional Pathway in Trabecular Meshwork Cells. *Invest Ophth Vis Sci* 59: 1969–1984.
34. Kim, Y. J., S. Narayanan, and K. O. Chang. 2010. Inhibition of influenza virus replication by plant-derived isoquercetin. *Antivir Res* 88: 227–235.

35. Chi, Y., Y. F. Zhu, T. Wen, L. B. Cui, Y. Y. Ge, Y. J. Jiao, T. Wu, A. H. Ge, H. Ji, and K. Xu, et al. 2013. Cytokine and Chemokine Levels in Patients Infected With the Novel Avian Influenza A (H7N9) Virus in China. *J Infect Dis* 208: 1962–1967.
36. Liu, Y. X., C. Zhang, F. M. Huang, Y. Yang, F. X. Wang, J. Yuan, Z. Zhang, Y. H. Qin, X. Y. Li, and D. D. Zhao, et al. 2020. Elevated plasma levels of selective cytokines in COVID-19 patients reflect viral load and lung injury. *Natl Sci Rev* 7: 1003–1011.
37. Korteweg, C., and J. A. Gu. 2010. Pandemic influenza A (H1N1) virus infection and avian influenza A (H5N1) virus infection: a comparative analysis. *Biochem Cell Biol* 88: 575–587.
38. Xu, C. L., L. B. Dong, L. Xin, Y. Lan, Y. K. Chen, L. M. Yang, and Y. L. Shu. 2009. Human avian influenza A (H5N1) virus infection in China. *Sci China Ser C* 52: 407–411.
39. Ngamsri, K. C., R. Wagner, I. Vollmer, S. Stark, and J. Reutershan. 2010. Adenosine Receptor A1 Regulates Polymorphonuclear Cell Trafficking and Microvascular Permeability in Lipopolysaccharide-Induced Lung Injury. *J Immunol* 185: 4374–4384.
40. Shen, Z., Z. Chen, X. Li, L. Xu, W. Guan, Y. Cao, Y. Hu, and J. Zhang. 2014. Host immunological response and factors associated with clinical outcome in patients with the novel influenza A H7N9 infection. *Clin Microbiol Infec* 20: O493–O500.
41. Punsmann, S., J. Hoppe, R. Klopfleisch, and M. Venner. 2020. *Acute interstitial pneumonia in foals: A severe, multifactorial syndrome with lung tissue recovery in surviving foals*. Equine Vet J.
42. Reynolds, H. Y. 2005. Lung inflammation and fibrosis - An alveolar macrophage-centered perspective from the 1970s to 1980s. *Am J Resp Crit Care* 171: 98–102.
43. SchultzCherry, S., and V. S. Hinshaw. 1996. Influenza virus neuraminidase activates latent transforming growth factor beta. *J Virol* 70: 8624–8629.
44. Chrostek, L., and A. Panasiuk. 2014. Liver fibrosis markers in alcoholic liver disease. *World J Gastroentero* 20: 8018–8023.
45. Horan, G. S., S. Wood, V. Ona, D. J. Li, M. E. Lukashev, P. H. Weinreb, K. J. Simon, K. Hahm, N. E. Allaire, and N. J. Rinaldi, et al. 2008. Partial inhibition of integrin alpha v beta 6 prevents pulmonary fibrosis without exacerbating inflammation. *Am J Resp Crit Care* 177: 56–65.
46. Passos, I. C., M. P. Vasconcelos-Moreno, L. G. Costa, M. Kunz, E. Brietzke, J. Quevedo, G. Salum, P. V. Magalhaes, F. Kapczinski, and M. Kauer-Sant'Anna. 2015. Inflammatory markers in post-traumatic stress disorder: a systematic review, meta-analysis, and meta-regression. Lancet Psychiat *2*, 1002–1012.
47. Jaakkola, P., D. R. Mole, Y. M. Tian, M. I. Wilson, J. Gielbert, S. J. Gaskell, A. von Kriegsheim, H. F. Hebestreit, M. Mukherji, and C. J. Schofield, et al. 2001. Targeting of HIF-alpha to the von Hippel-Lindau ubiquitylation complex by O-2-regulated prolyl hydroxylation. *Science* 292: 468–472.
48. Deshmane, S. L., R. Mukerjee, S. S. Fan, L. Del Valle, C. Michiels, T. Sweet, I. Rom, K. Khalili, J. Rappaport, and S. Amini, et al. 2009. Activation of the Oxidative Stress Pathway by HIV-1 Vpr Leads to Induction of Hypoxia-inducible Factor 1 alpha Expression. *J Biol Chem* 284: 11364–11373.

49. Shi, Y. F., C. C. Fong, Q. Zhang, P. Y. Cheung, C. H. Tzang, R. S. S. Wu, and M. S. Yang. 2007. Hypoxia induces the activation of human hepatic stellate cells LX-2 through TGF-beta signaling pathway. *Febs Lett* 581: 203–210.
50. Cramer, T., Y. Yamanishi, B. E. Clausen, I. Forster, R. Pawlinski, N. Mackman, V. H. Haase, R. Jaenisch, M. Corr, and V. Nizet, et al. 2003. HIF-1 alpha is essential for myeloid cell-mediated inflammation. *Cell* 112: 645–657.
51. Guo, X. K., Z. Q. Zhu, W. J. Zhang, X. X. Meng, Y. Zhu, P. Han, X. H. Zhou, Y. W. Hu, and R. L. Wang. 2017. Nuclear translocation of HIF-1 alpha induced by influenza A (H1N1) infection is critical to the production of proinflammatory cytokines. Emerg Microbes Infec *6*.
52. Tolnay, A. E., C. R. Baskin, T. M. Tumpey, P. J. Sabourin, C. L. Sabourin, J. P. Long, J. A. Pyles, R. A. Albrecht, A. Garcia-Sastre, and M. G. Katze, et al. 2010. Extrapulmonary tissue responses in cynomolgus macaques (Macaca fascicularis) infected with highly pathogenic avian influenza A (H5N1) virus. *Arch Virol* 155: 905–914.
53. Casiraghi, C., T. Gianni, and G. Campadelli-Fiume. 2016. alpha v beta 3 Integrin Boosts the Innate Immune Response Elicited in Epithelial Cells through Plasma Membrane and Endosomal Toll-Like Receptors. *J Virol* 90: 4243–4248.
54. Walton, H. L., M. H. Corjay, S. N. Mohamed, S. A. Mousa, L. D. Santomenna, and T. M. Reilly. 2000. Hypoxia induces differential expression of the integrin receptors alpha(v beta 3) and alpha(v beta 5) cultured human endothelial cells. *J Cell Biochem* 78: 674–680.

Figures

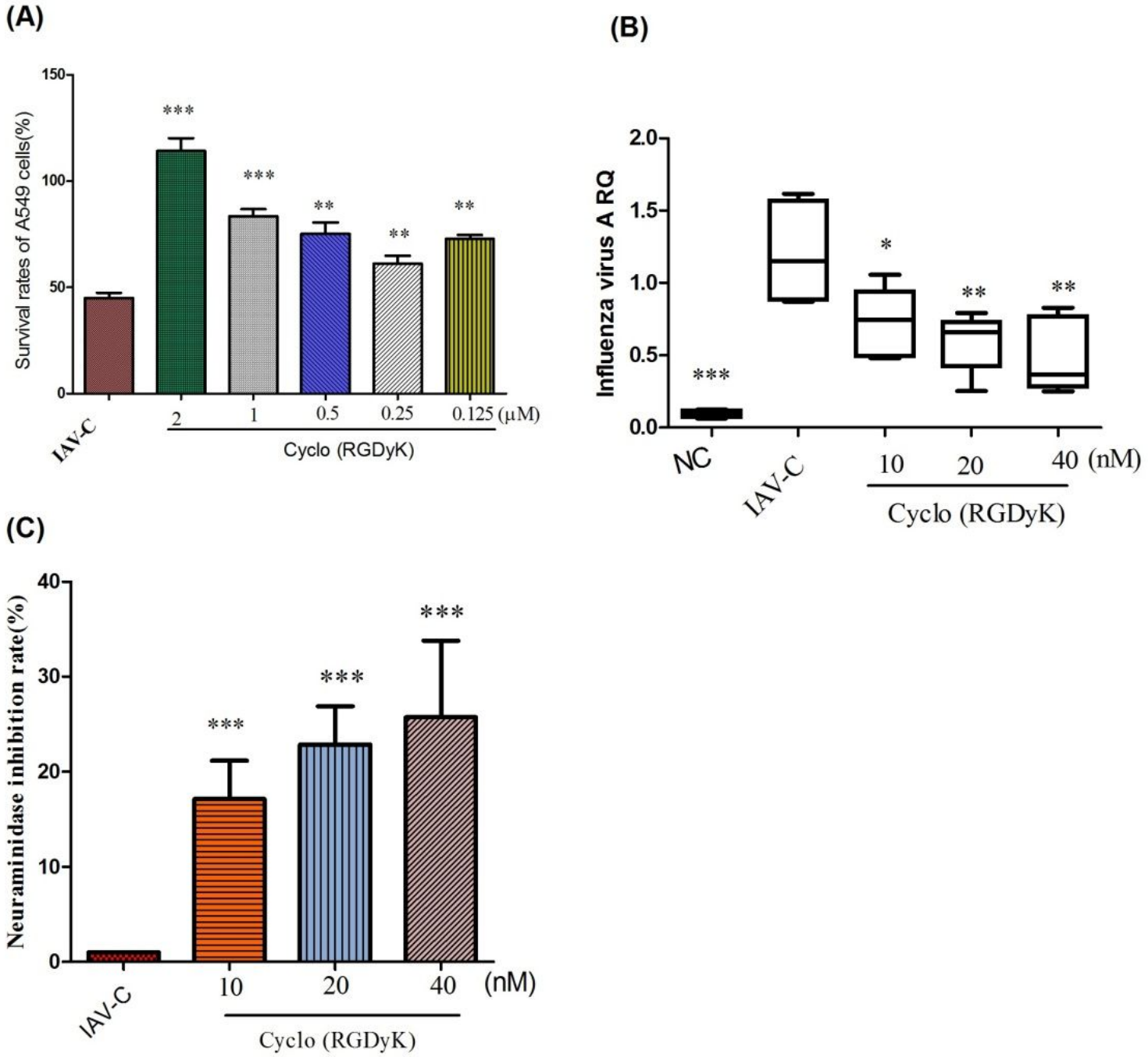

Figure 1

Evaluation of the anti-influenza abilities of Cyclo(RGDyK) in cells. (A) Inhibitory effects of Cyclo (RGDyK) on survival rate of infected cells; (B) Relative quantitation of influenza A virus in cells; (C)Neuraminidase activity inhibition rate. Cells(1×105/well) were treated with various amounts of Cyclo (RGDyK) at the same time as inoculation with FM1/H1N1 suspension (100 TCID50/well). After incubation for 72h at 37°C and 5% CO2, the cells were stained with 0.5% MTT. The cell viability was determined by the MTT assay at a wavelength of 490nm. Each concentration took up three wells during each assay independent determinations were carried out. **p <0.01, ***p <0.001, compared to IAV-C group.

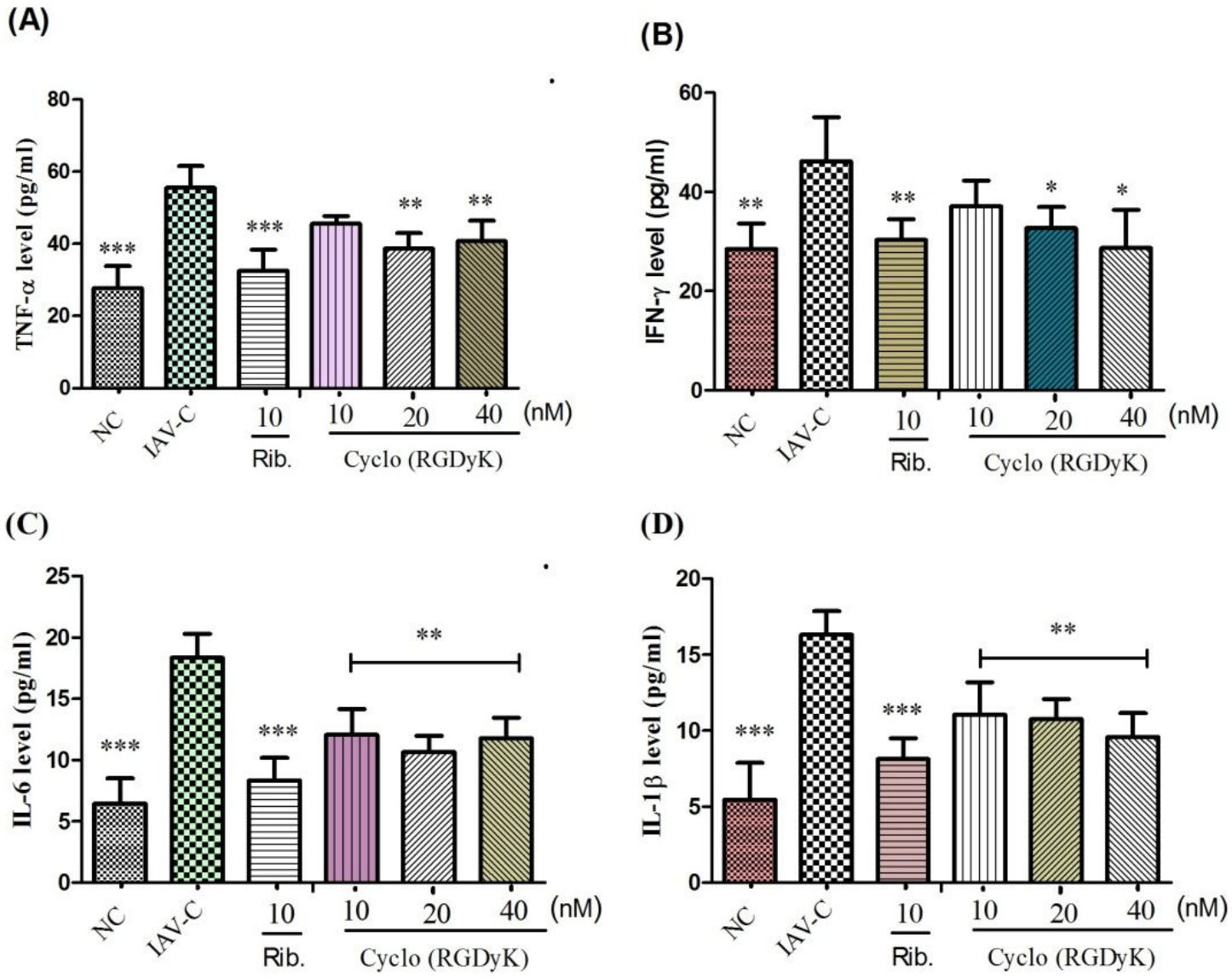

Figure 2

Effects of Cyclo (RGDyK) on proinflammatory cytokine production in cells infected by IAV. (A) The level of TNF-α in cells; (B)The level of IFN-γ in cells;(C)The level of IL-6 in cells, (D) The level of IL-1β in cells. Cells(1×105/well) were treated with various amounts of Cyclo (RGDyK) at the same time as inoculation with FM1/H1N1 suspension (100 TCID50/well). After incubation for 72h at 37°C and 5% CO2, the levels of cytokines were measured by ELISA assay. Data were presented as mean ± SD. Asterisks denote the significance levels: * p <0.01; ** p <0.01; *** p <0.001, compared with IAV-C group.

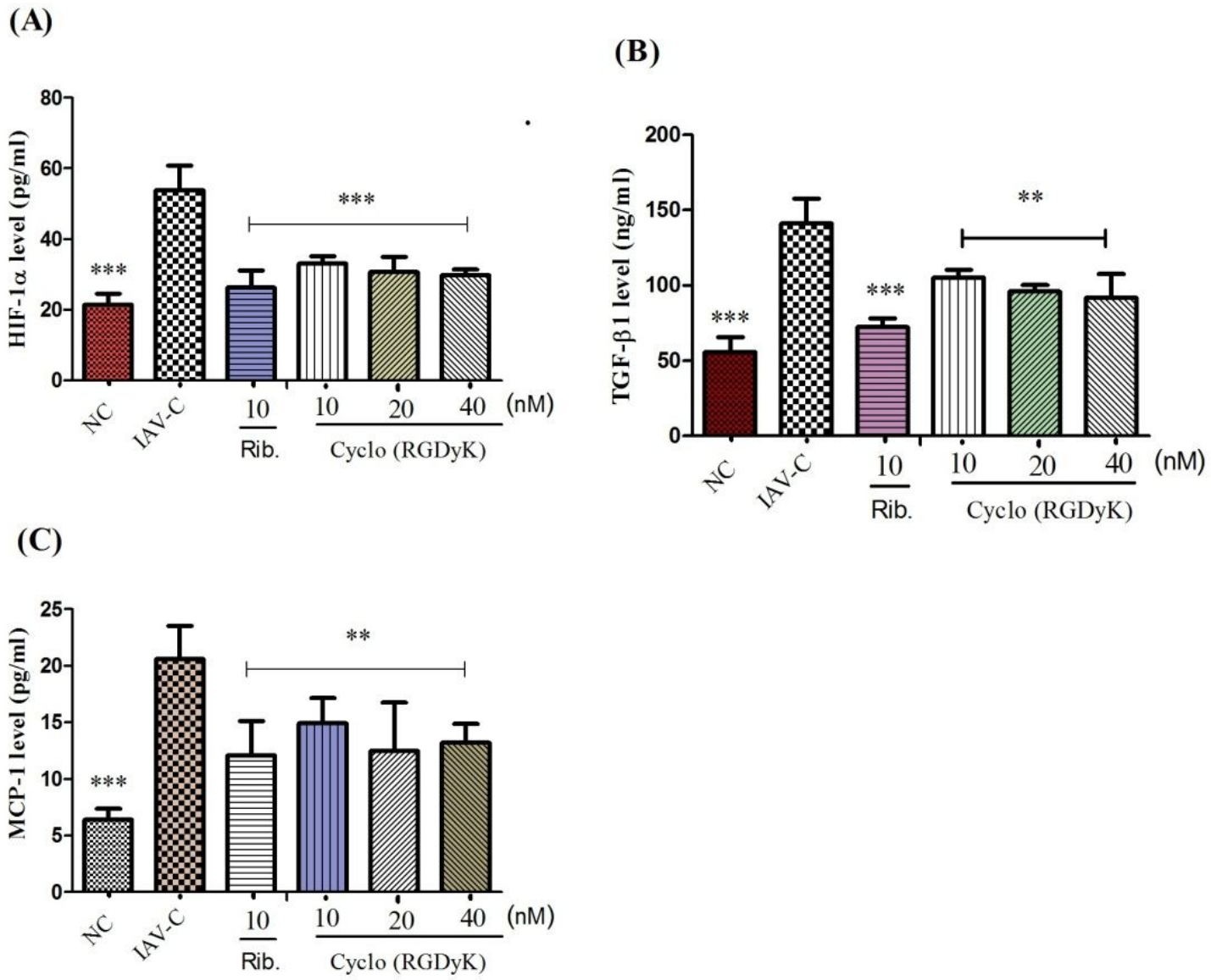

Figure 3

Effects of Cyclo (RGDyK) on cytokine production in cells infected by IAV. (A) The level of HIF-1α in cells; (B)The level of TGF-β1in cells;(C)The level of MCP-1 in cells. Cells(1×105/well) were treated with various amounts of Cyclo (RGDyK) at the same time as inoculation with FM1/H1N1 suspension (100 TCID50/well). After incubation for 72h at 37°C and 5% CO2, the levels of cytokines were measured by ELISA assay. Data were presented as mean ± SD. Asterisks denote the significance levels: * p <0.01; ** p <0.01; *** p <0.001, compared with IAV-C group.

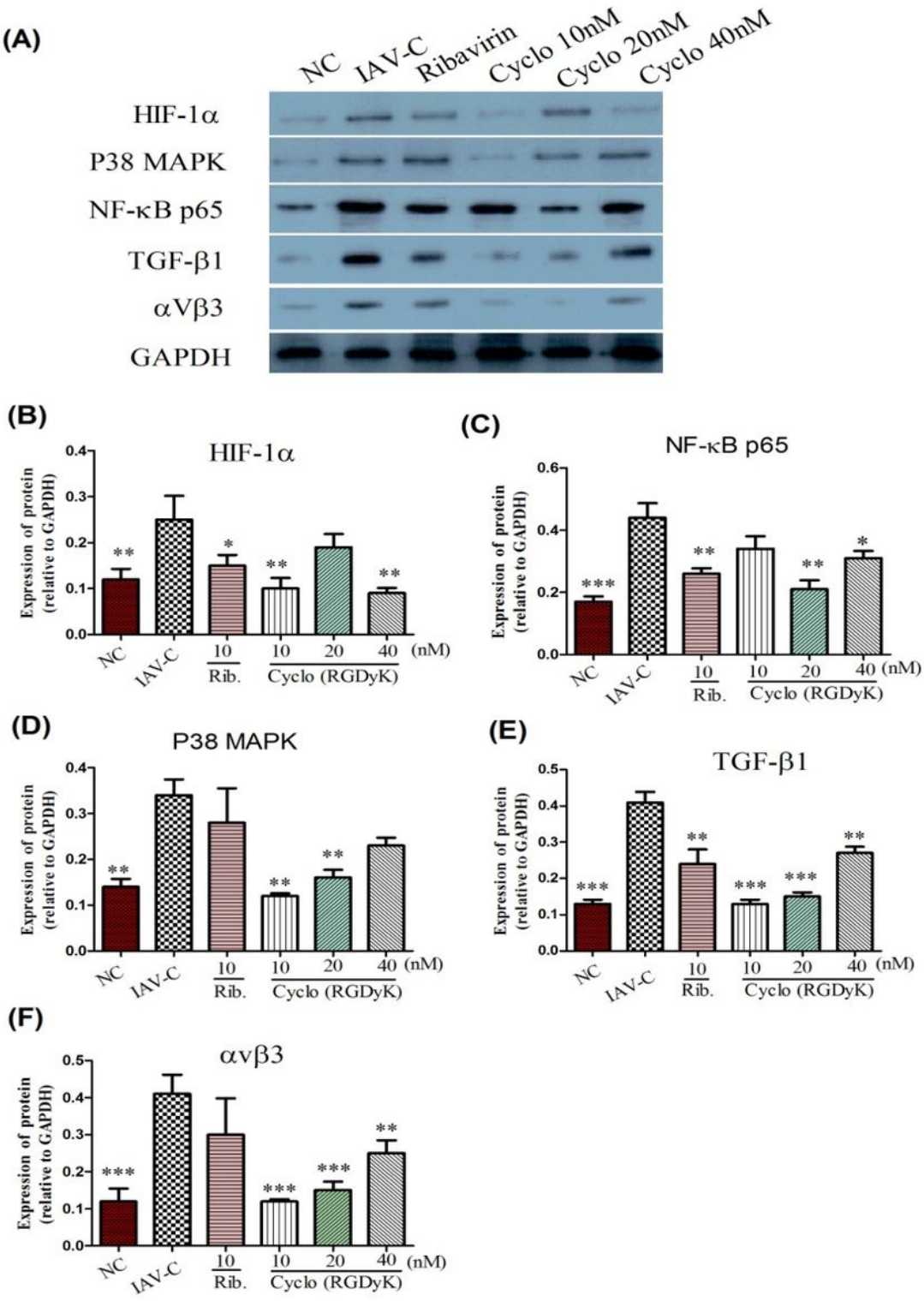

Figure 4

Effect of Cyclo (RGDyK) on protein expression in cells infected with IAV by western blot analysis(n=5). (A) Representative page of proteins expression by western blotting;(B) Semi-quantitative analysis of HIF-1α protein; (C) Semi-quantitative analysis of NF-κB p65 protein; (D) Semi-quantitative analysis of p38MAPK protein; (E) Semi-quantitative analysis of TGF-β1 protein; (F) Semi-quantitative analysis of αVβ3 protein. Cells(1×105/well) were treated with various amounts of Cyclo (RGDyK) at the same time as inoculation

with FM1/H1N1 suspension (100 TCID50/well). After incubation for 72h at 37℃ and 5% CO2, the expression level of proeteins were measured by western blot assay.GAPDH protein was used as a loading control.Values are mean ± SD. Asterisks denote the significance levels: * p <0.05; ** p <0.01; *** p <0.001, compared with IAV-C group.

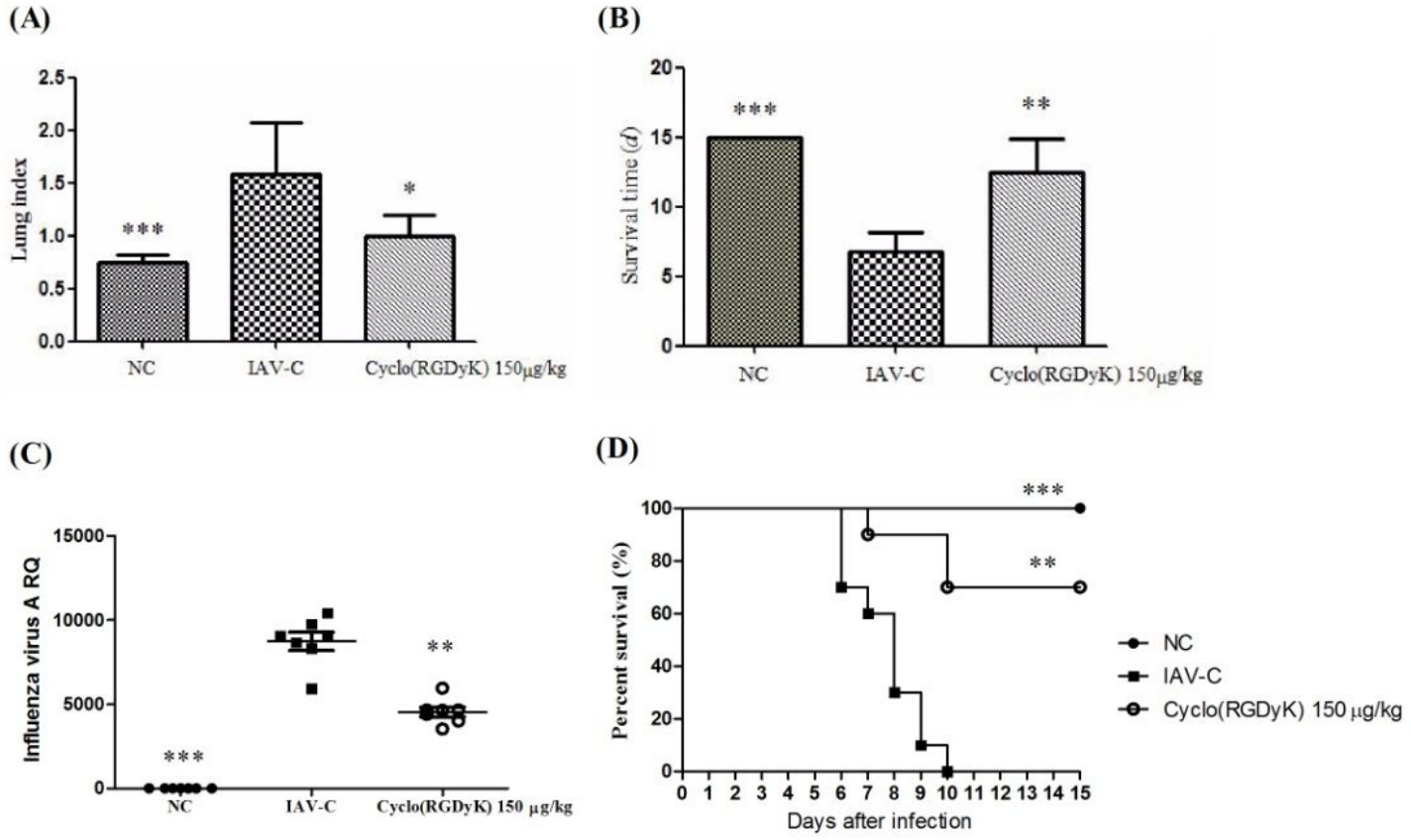

Figure 5

The anti-influenza activity of activity of Cyclo(RGDyK) in mice infected by IAV. (A) Lung index; (B)Survival time; (C) Relative quantitation of influenza A virus in lung;(D) Survival rate. Mice were infected with 5 LD50 of FM1/H1N1 and treated with Cyclo (RGDyK) (i.p.) once a day for 5 days. Clinical signs were observed for 14 days (n=10). Values are mean ± SD. Asterisks denote the significance levels: *p< 0.05; **p< 0.01; *** p< 0.001, compared with IAV-C group.

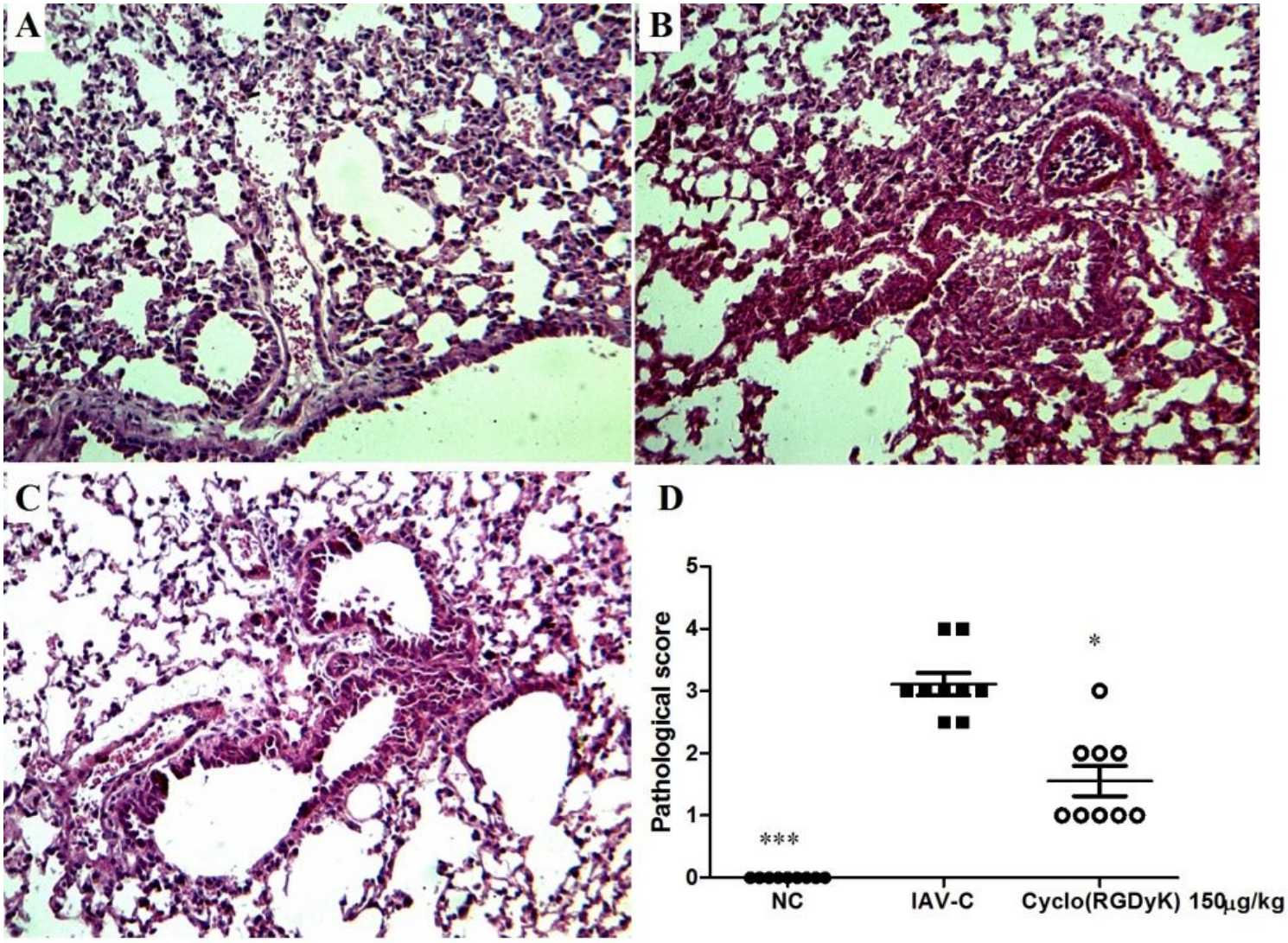

Figure 6

Pathologies of lungs of mice infected with IAV (HE,× 100). (A) Pathological changes of lung tissues in NC group; (B) Pathological changes of lung tissues in IAV-C group; (C) Pathological changes of lung tissues in Cyclo (RGDyK) group; (D) Pathological scores. Mean score ± SD, n=5 mice per group),*p<0.05 , ***p<0.001, compared to the IAV-C group.

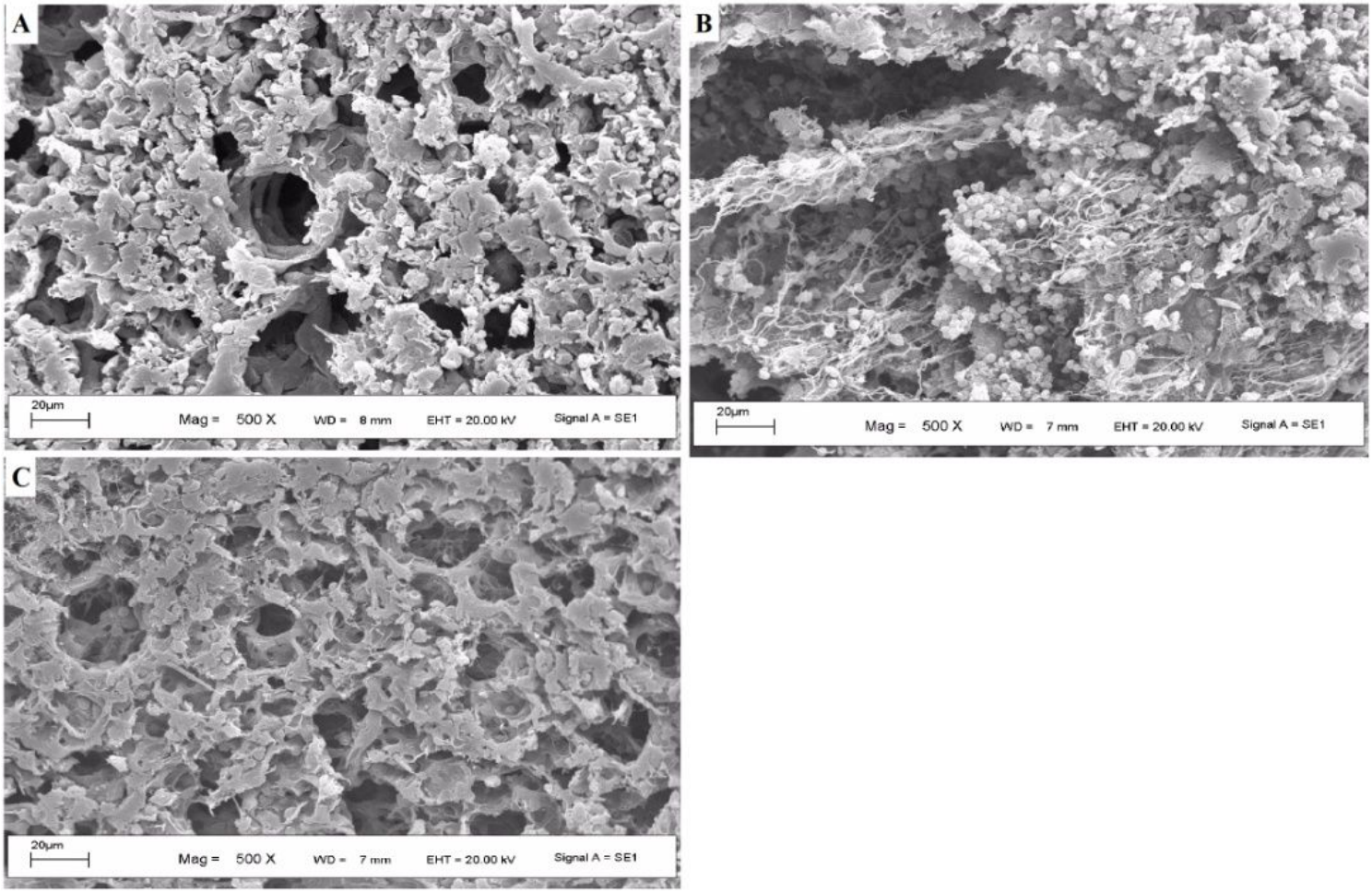

Figure 7

Ultrastructural changes of lung tissues mice infected with IAV (electron microsopy, × 500) (A) Ultrastructural changes of lung tissues in NC group; (B) Ultrastructural changes of lung tissues in IAV-C group; (C) Ultrastructural changes of lung tissues in Cyclo (RGDyK) group. n=5 mice per group.

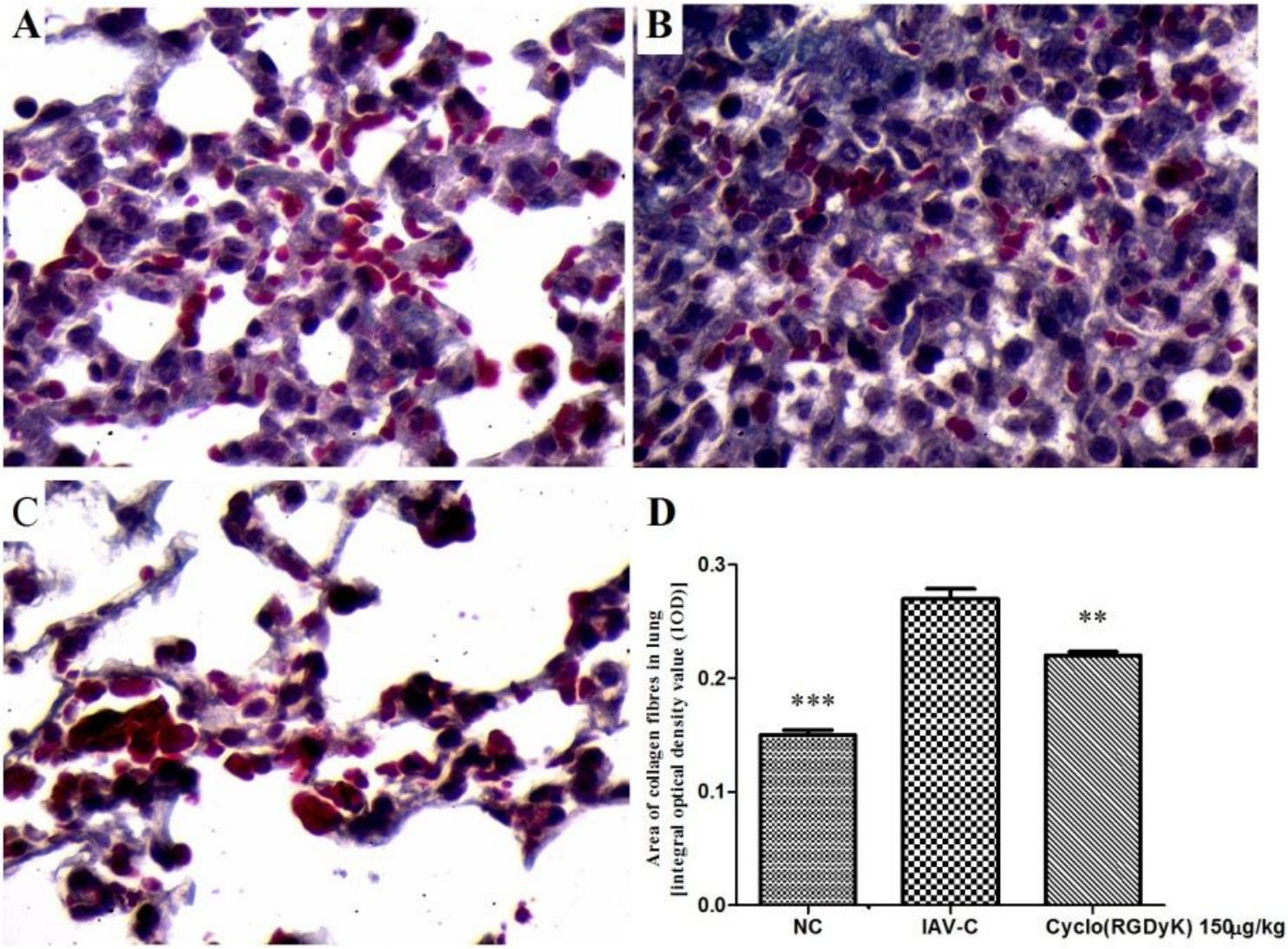

Figure 8

Effects of Cyclo (RGDyK) against lung fibrosis in mice induced by IAV based on Masson staining (×100). (A) Pathological changes of lung tissues in NC group; (B) Pathological changes of lung tissues in IAV-C group; (C) Pathological changes of lung tissues in 150μg/kg Cyclo (RGDyK) group; (D) Area of collagen fibers in lung. Data were presented as mean ± SD. Asterisks denote the significance levels: **p <0.01 and ***p <0.001, compared with IAV-C group.

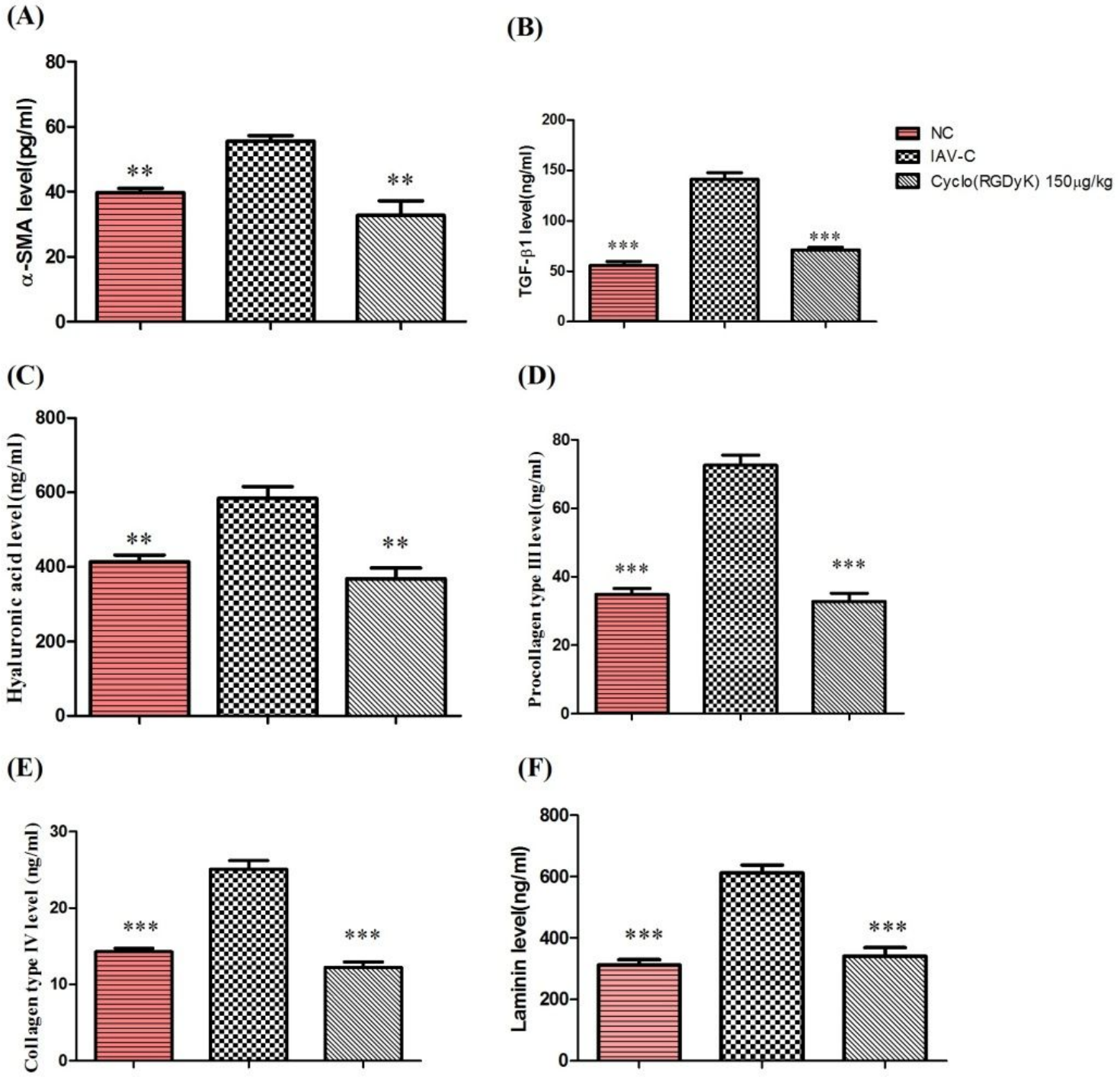

Figure 9

Effects of Cyclo (RGDyK) on levels of fibrotic markers in ALI mice induced by IAV. (A)α-SMA level in serun; (B)TGF-β1 level in serun ; (C)HA level in serun; (D)PCIII level in serun; (E)PCIV level in serun; (F)LN level in serun.Values are mean ± SD. **p <0.01, ***p <0.001, versus IAV-C group. HA, hyaluranic acid; LN, lamin; PCIII, procollagen type III; IV-C, collagen type IV; TGF-β1, Transforming growth factor beta 1; α-SMA, alpha smooth muscle actin.

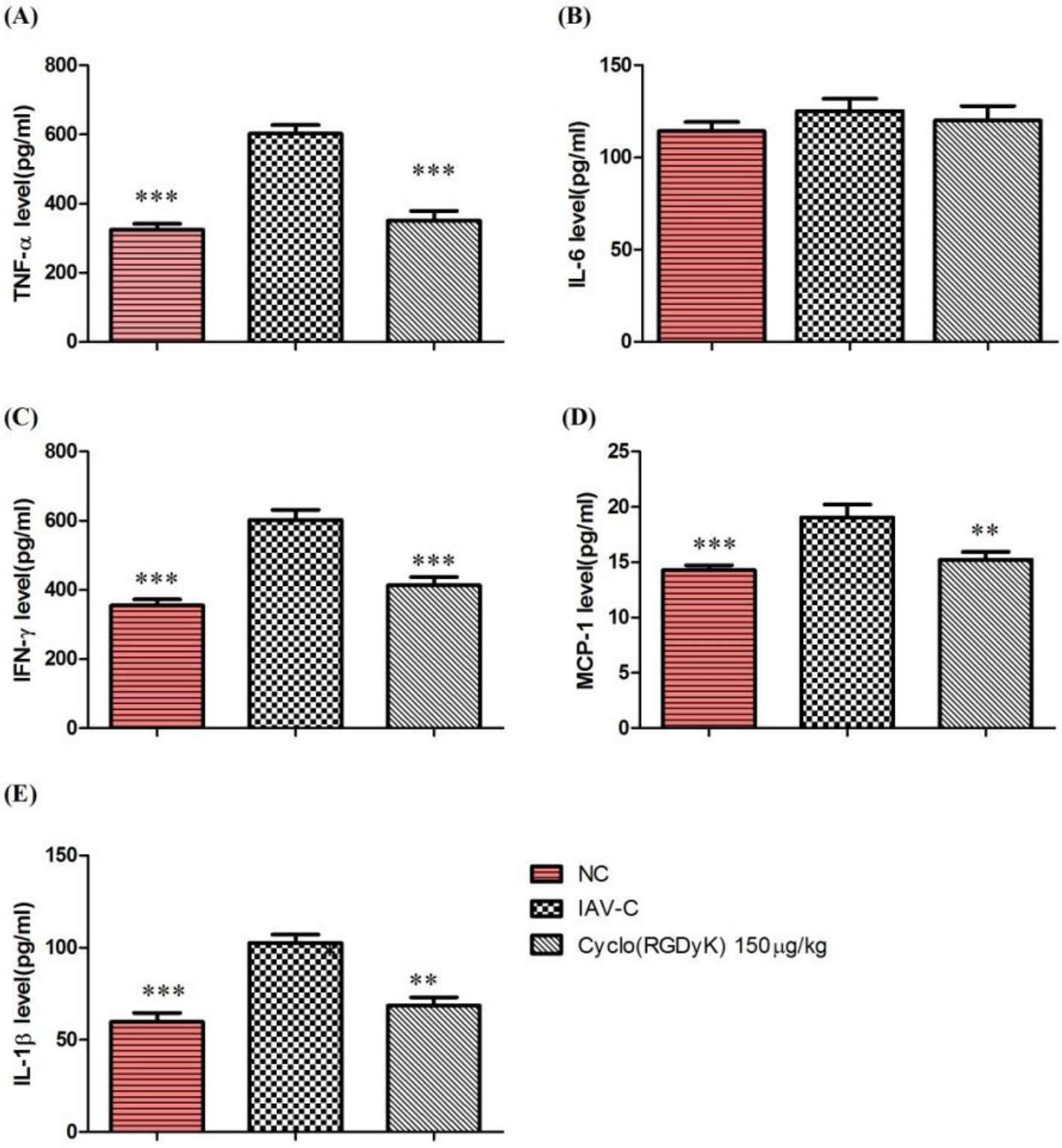

Figure 10

Effects of Cyclo (RGDyK) on proinflammatory cytokine production in IAV-induced ALI mice.. (A) The level of TNF-alpha in lung homogenate; (B)The level of IL-6 in lung homogenate;(C)The level of IFN-gamma in lung homogenate, (D) The level of MCP-1 in lung homogenate; (E) The level of IL-1beta in lung homogenate. Lung tissues were prepared from mice 6d after IAV stimulation. The levels of cytokines were

measured by ELISA assay. Data were presented as mean ± SD. Asterisks denote the significance levels: ** p <0.01; *** p <0.001, compared with IAV-C group.

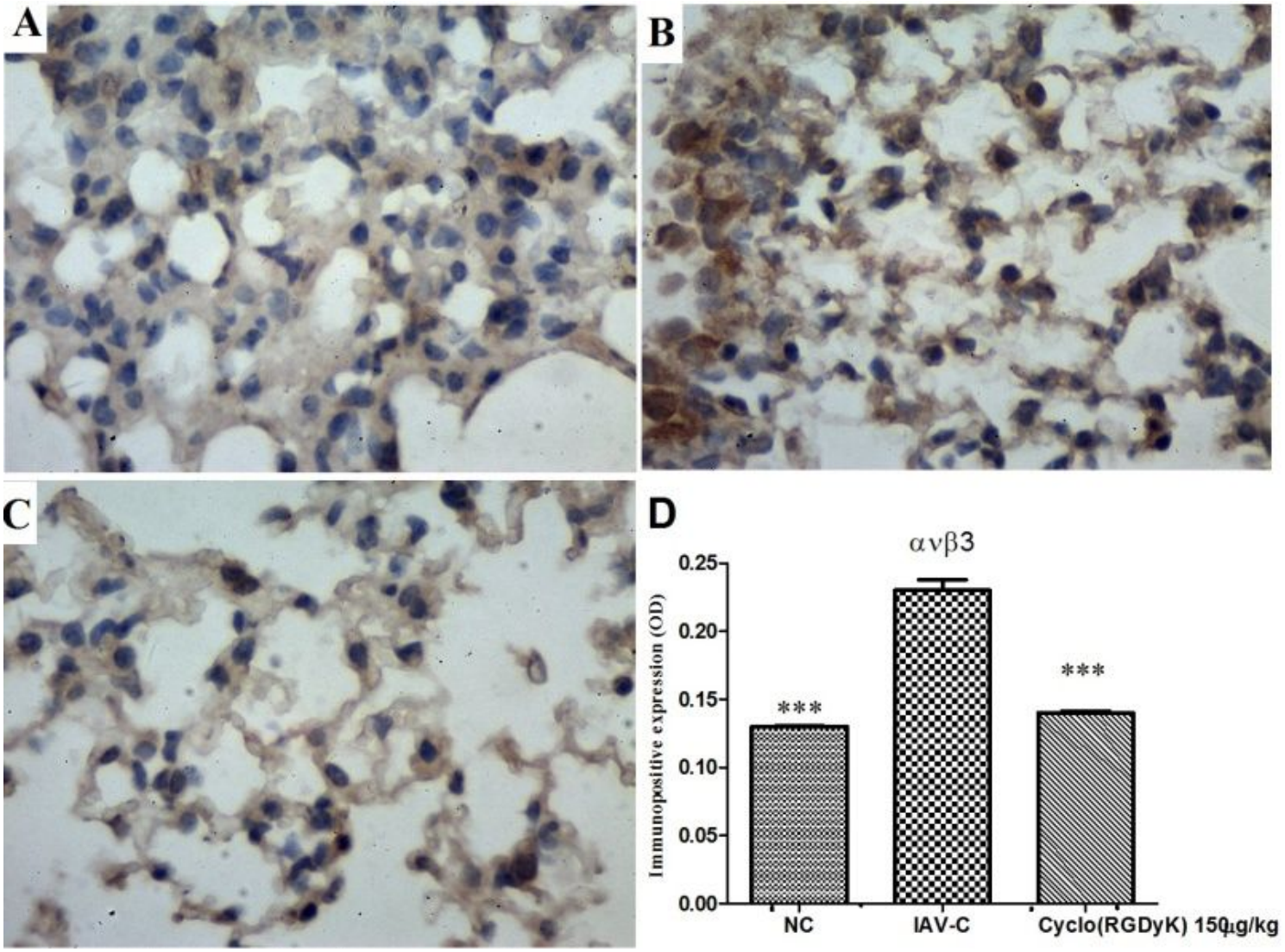

Figure 11

Effect of Cyclo (RGDyK) on αvβ3 signaling pathway expression in ALI in mice infected with IAV by immunohistochemical analysis (n=5).(A) Representative page of proteins expression in NC group; (B) Representative page of proteins expression in IAV-C group; (C) Representative page of proteins expression in Cyclo (RGDyK) group; (D) Semi-quantitative analysis of immunopositive expression.Values are mean ± SD. Asterisks denote the significance levels: *** p <0.001, compared with IAV-C group.

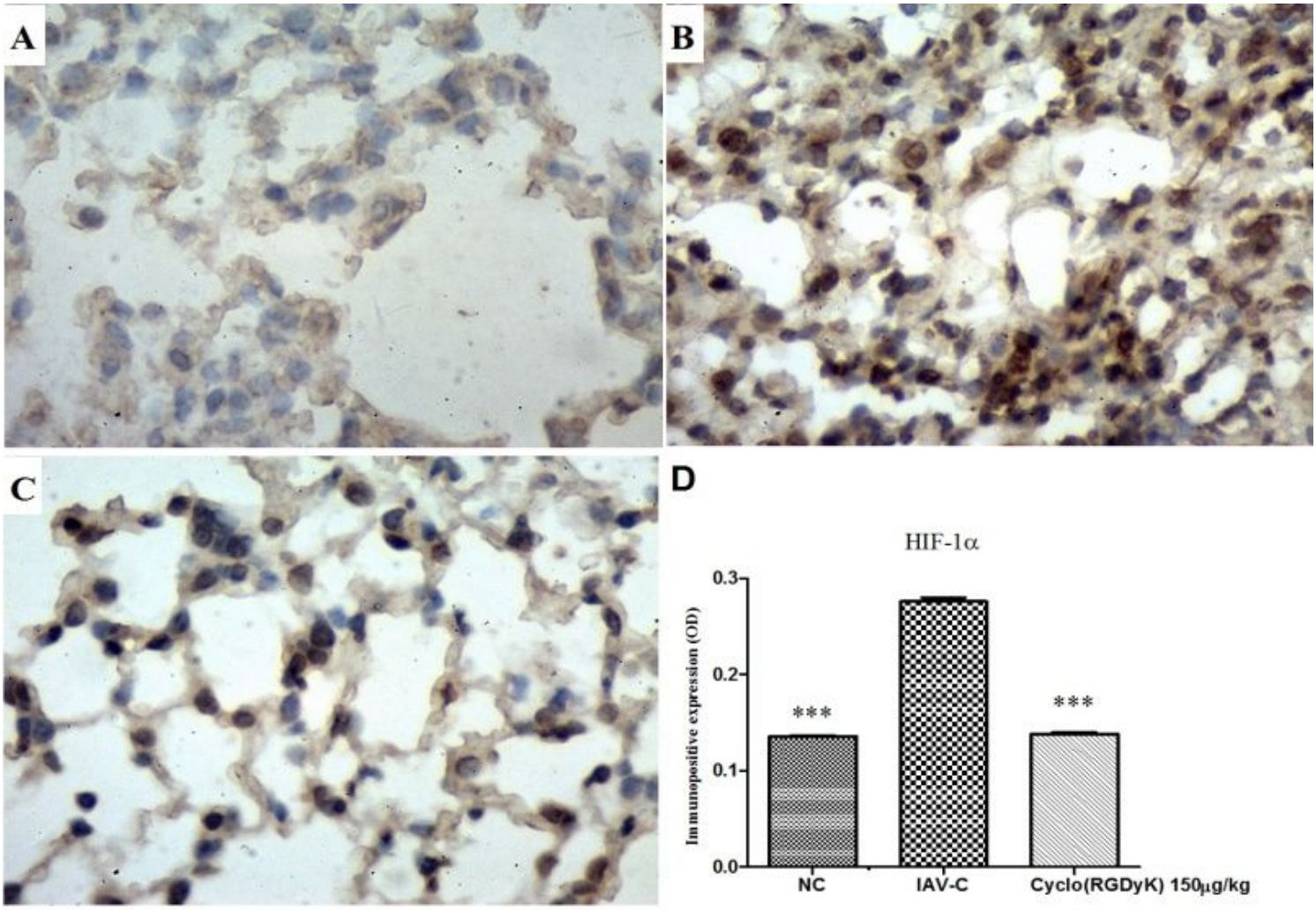

Figure 12

Effect of Cyclo (RGDyK) on HIF-1α signaling pathway expression in ALI in mice infected with IAV by immunohistochemical analysis (n=5). (A) Representative page of proteins expression in NC group; (B) Representative page of proteins expression in IAV-C group; (C) Representative page of proteins expression in Cyclo (RGDyK) group; (D) Semi-quantitative analysis of immunopositive expression.Values are mean ± SD. Asterisks denote the significance levels: *** p <0.001, compared with IAV-C group.

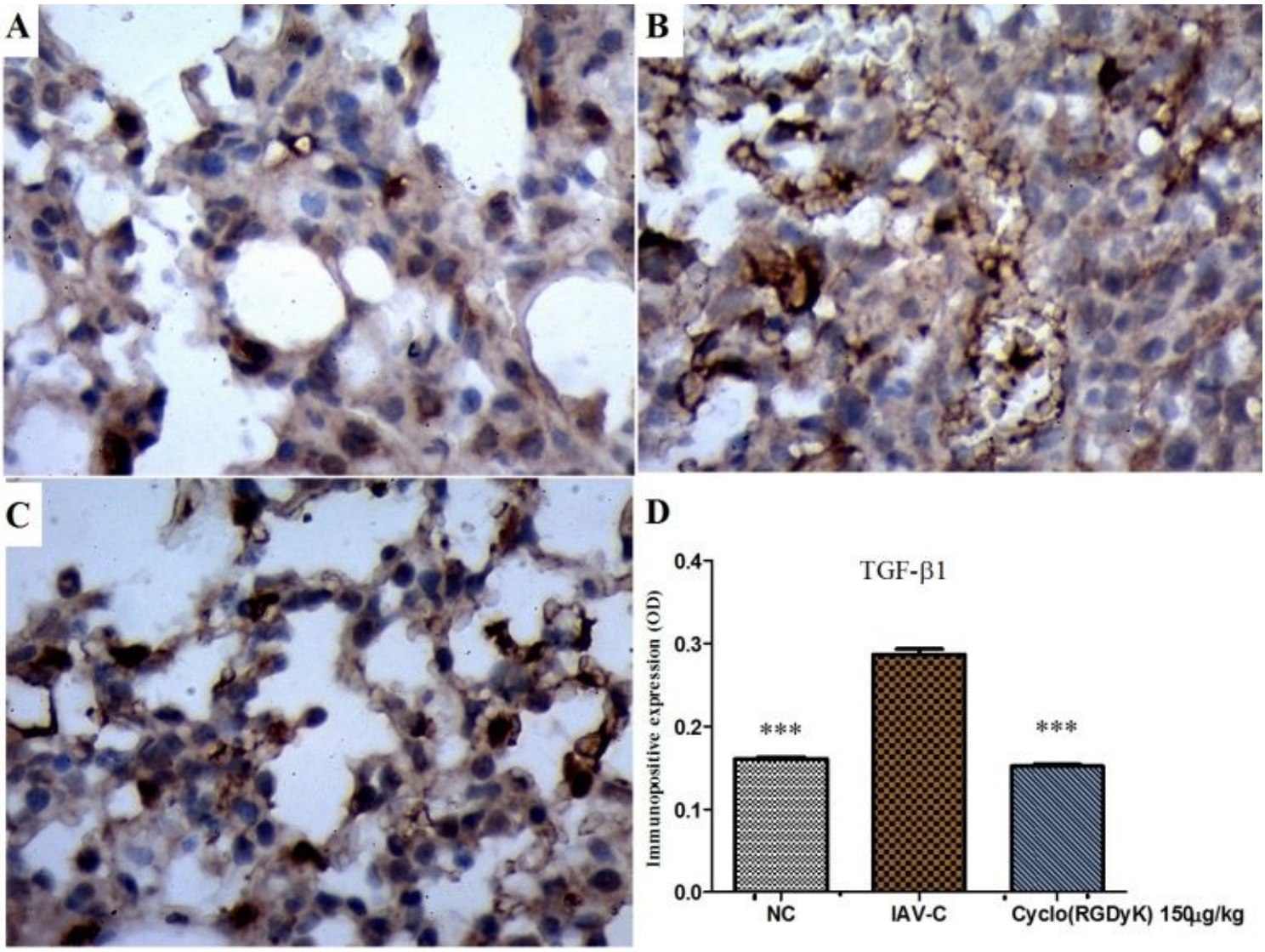

Figure 13

Effect of Cyclo (RGDyK) on TGF-β1 signaling pathway expression in ALI in mice infected with IAV by immunohistochemical analysis (n=5). (A) Representative page of proteins expression in NC group; (B) Representative page of proteins expression in IAV-C group; (C) Representative page of proteins expression in Cyclo (RGDyK) group; (D) Semi-quantitative analysis of immunopositive expression. Values are mean ± SD. Asterisks denote the significance levels: *** p <0.001, compared with IAV-C group.